J|A|C|S
ARTICLES

Published on Web 09/24/2009

Time-Resolved X-ray Diffraction of the Photochromic α-Styrylpyrylium Trifluoromethanesulfonate Crystal Films Reveals Ultrafast Structural Switching

Jörg Hallmann,[†] Wolfgang Morgenroth,[‡,§] Carsten Paulmann,[‡,||] Jav Davaasambuu,[†] Qingyu Kong,[⊥] Michael Wulff,[⊥] and Simone Techert*[,†]

IFG Structural Dynamics of (Bio)chemical Systems, Max Planck Institute for Biophysical Chemistry, 37070 Göttingen, Germany, HASYLAB at DESY, Notkestrasse 85, 22607 Hamburg, Germany, Institut für Geowissenschaften, Facheinheit Mineralogie, Abt. Kristallographie, Universität Frankfurt, Altenhöferallee 1, 60438 Frankfurt am Main, Germany, Mineralogisch-Petrographisches Institut, Universtität Hamburg, Grindelallee 48, 20146 Hamburg, Germany, and European Synchrotron Radiation Facility, 38043 Grenoble, France

Received July 3, 2009; E-mail: stecher@gwdg.de

Abstract: The ultrafast structural dynamics of the [2+2] photocycloaddition of α-styrylpyrylium trifluoromethanesulfonate (TFMS) has been studied in great detail. During the photoreaction, optical and infrared spectroscopy confirms that crystals of α-styrylpyrylium change color. Since the reaction is reversible, it has been suggested to be used as an organic holographic storage device. The present photocrystallographic studies (with high spatial resolution) allow for an electron density analysis of the overall reaction kinetics, revealing the mechanism of bond-breaking and bond-formation. It could furthermore be proved how the reaction is influenced by the rearrangement of the surrounding moieties. Picosecond time-resolved X-ray diffraction studies allow for the monitoring the photoreaction in crystalline thin films under experimental conditions where the transformation times are greatly enhanced. These investigations are discussed in the context of the photocrystallographic results. It has been found that α-styrylpyrylium TFMS undergoes an ultrafast photoreaction to the dimer product state and back-reaction to the monomer reactant state which is temperature driven. The present experiments indicate that TFMS reacts on time scales which are the fundamental limiting ones of two-quantum systems and therefore has the potential to be used as an ultrafast organic molecular switcher.

Introduction

During the second half of the 20th century, the systematic investigation of solid-state reactions and the growing number of examples of solid-state reactions explored have witnessed to their value not only because they are much more selective concerning the product distribution but also because they are environmental friendly and proved to be useful in the context of "green" chemistry. The rationalization of photoreactions in the solid state was founded by various pioneering works, including the introduction of the topochemical principle and activation of volume-confined solid-state reactions.[1−6]

Solid-state photochemical reactions are highly dependent on the geometry of the reacting compounds and their products. Much experimental work has been undertaken to understand the thermodynamical properties of solids undergoing solid-state reactions,[5−31] the influence of the spatial arrangements of the

[†] Max Planck Institute for Biophysical Chemistry.
[‡] HASYLAB at DESY.
[§] Universität Frankfurt.
[||] Universtität Hamburg.
[⊥] European Synchrotron Radiation Facility.

(1) Hertel, F. *Z. Elektrochem.* **1931**, *37*, 536.
(2) Cohen, M. D.; Schmidt, G. M. J.; Sonntag, J. *J. Chem. Soc.* **1964**, 2000.
(3) Zimmermann, H. E.; Sebek, P. *J. Am. Chem. Soc.* **1997**, *119*, 3667.
(4) McBride, J. M. *Acc. Chem. Res.* **1983**, *16*, 304.
(5) Weiss, R. G.; Ramamurthy, V.; Hammond, G. S. *Acc. Chem. Res.* **1993**, *26*, 530.
(6) Wegner, G. *Z. Naturforsch.* **1969**, *24b*, 824.
(7) Nakanishi, H.; Jones, W.; Thomas, J. M.; Hursthouse, M. B.; Motevalli, M. *J. Phys. Chem.* **1981**, *85*, 3636.
(8) Harris, K. D. M.; Thomas, J. M. *J. Solid State Chem.* **1991**, *93*, 197.
(9) Davaasambuu, J.; Techert, S. *J. Phys. D: Appl. Phys.* **2005**, *38*, A204.
(10) Davaasambuu, J.; Busse, G.; Techert, S. *J. Phys. Chem. A* **2006**, *110*, 3261.
(11) Busse, G.; Tschentscher, T.; Plech, A.; Wulff, M.; Frederichs, B.; Techert, S. *Faraday Discuss.* **2002**, *122*, 105.
(12) Zimmermann, H. E.; Nesterov, E. E. *Acc. Chem. Res.* **2002**, *35*, 77.
(13) Gavezzoti, A.; Simonetta, M. *Chem. Rev.* **1982**, *82*, 1.
(14) Ohashi, Y.; Tomotake, Y.; Akira, U.; Sasada, Y. *J. Am. Chem. Soc.* **1986**, *108*, 1196.
(15) Ramamurthy, V.; Venkatesan, K. *Chem. Rev.* **1987**, *87*, 433.
(16) Legrand, V.; Pillet, S; Weber, H. P.; Souhassou, M.; Letard, J.-F.; Guionneau, P.; Lecomte, C. *J. Appl. Crystallogr.* **2007**, *40*, 1076.
(17) Vorontsov, I. I.; Kovalevsky, A. Y.; Chen, Y.-S.; Graber, T.; Gembicky, M.; Novozhilova, I. V.; Omary, M. A.; Coppens, P. *Phys. Rev. Lett.* **2005**, *94*, 193003.
(18) Allen, F. H.; Mahon, M. F.; Raithby, P. R.; Shields, G. P.; Sparkes, H. A. *New J. Chem.* **2005**, *29*, 182.
(19) Techert, S.; Zachariasse, K. A. *J. Am. Chem. Soc.* **2004**, *126*, 5593.
(20) Srajer, V.; Teng, T.-Y.; Ursby, T.; Pradevard, C.; Ren, Z.; Adachi, S.; Schildkamp, W.; Bourgeois, D.; Wulff, M.; Moffat, K. *Science* **1996**, *274*, 1726–1729.
(21) Quevedo, W.; Petri, M.; Busse, G.; Techert, S. *J. Chem. Phys.* **2008**, *129*, 024502.

 10.1021/ja905484u CCC: $40.75

molecules within the lattice, their optimization (i.e., crystals dispersed in protic or aprotic solvent), or their temperature dependence.

An important advantage of understanding the reaction mechanism, the course of the reaction, and the reaction control factors is the ability to follow structural changes during reactions. From a general kinetic point of view, photoinduced solid-state reactions can be separated into two categories: reversible and irreversible reactions. Furthermore, one may distinguish between homogeneous single-crystal to single-crystal dimerization reactions[8,9] and heterogeneous dimerization reactions[7,10,11] where the long-range order is destroyed. Depending on the optical excitation conditions, the same kind of photodimerization can be homogeneous or heterogeneous.[2,31]

The mechanism of photodimerization is explained by the so-called topochemical principle. Since its first introduction in 1931,[1,2] topochemical reactions in the crystalline state have been a permanent topic of experimental studies in different solid-state schools. According to this principle, crystal systems with two reacting molecules closer than 4.2 Å (in more detail, if the distance *r* between the two reaction double bond systems of the reactants is smaller than 4.2 Å) undergo a photoaddition reaction. If the intermolecular distance is bigger than 4.2 Å, the crystal is photoinactive. This principle explains why one and the same molecular system does or does not undergo a photoaddition reaction, depending on the morphology of the crystal yielded. Organic molecules tend to polymorphism; therefore, depending on their packing, the same molecular system in the crystalline phase may or may not be photoactive. Although several exceptions to this rule have been reported,[32,33] the topochemical principle is an appropriate guideline to predict the possibility of photoactivity in a molecular substance.

Since these first pioneering reports, the understanding of how crystal packing properties of organic solids influence crystal reactivity during photochemical reactions has continuously improved.[3,12] In particular, the progress in theoretical models coupled with increased computer simulation capabilities makes it possible now to simulate lattice-dictated solid-state reactions on a high-level *ab initio* quantum mechanical/molecular mechanical (QM/MM) approach or a pure MM approach. The simulations enable an accurate mechanistic description of photoinduced type-B rearrangements in bicyclohexenone crystals,[3] as one example, or they can be used to describe the role of cage effects, local stress, and friction (in the form of hindered rotations) on the photoreaction of crystalline benzoyl peroxide dissociation,[12] as another example.

Going back to the early work of Cohen and Schmidt and their concept of a reaction cavity, chromophores in crystals can be visualized as existing in rigid, three-dimensional cavities formed by their nearest neighbors.[2] As the central molecule reacts, its geometry changes within the cavity. Reactions that involve minor changes in reactant geometry are topochemically allowed, since they progress without restriction from the cavity walls. Reactions with transition-state geometries that do not fit within the cavity are strongly disfavored.[13,14] The effect of attractive and repulsive van der Waals forces on the energies of the reactant and product states, respectively, has intensively been investigated in ref 15.

Photocrystallography is the method of choice to study photoreactions in the solid state.[16−18] The formation of optically created short-living transient structures or intermediates which ultimately direct the reaction pathway is a common feature of all photocrystallographic reactions. Just recently it became possible to investigate the structure of these intermediates by time-resolved laser pump/X-ray probe experiments as they are provided by time-resolved X-ray diffraction techniques.[19] The short X-ray pulses are either generated by plasma sources in laboratories or provided as brilliant picosecond X-ray pulses at available synchrotron sources. So far, most reactions studied by time-resolved X-ray diffraction make use of the repetitive character of the pump/probe experiment and are of reversible nature.[20]

Time-resolved X-ray diffraction based on the optical laser pulse pump/X-ray probe scheme is a unique and powerful method to distinguish between these different reactions since crystallography probes the structural rearrangements of the *bulk* under illumination.[21] In contrast, time-resolved spectroscopy gives evidence of the *local* structural changes.[22,23] Though a broad variety of heterogeneous dimerization reactions are found, homogeneous solid-state reactions are rare. In some cases, the crystal structures of a solid solution containing both the substrate and the product were analyzed structurally;[24,25] i.e., the structural changes in photochromic salicylideneaniline crystals using two-photon excitation were observed by X-ray diffraction of a single-crystal,[26] and the structures of the light-induced radical pair from a hexaarylbiimidazolyl derivative together with its ground-state substrate were determined by X-ray diffraction of a single-crystal, too.[27]

Photoinduced processes in organic single crystals have been studied for a long time, and in recent years their potential for possible technical applications in a variety of photosensitive devices has made them the focus of much research.[28,29] In synthetic chemistry for example, template-controlled reactions in the organic solid state can be used to construct a molecule that functions as an organic building unit of both a metal−organic polyhedron and a polygon.[30] In this way, it is possible to simulate two-step processes consisting of a template-directed synthesis step and a self-assembly step in order to construct large, functional self-assembled structures. Photoinduced solid-state reactions are ideal for initiating at least one of these steps.

In this work we aim to prove the ultrafast photoinduced structural switching process of a [2+2] photodimerization reaction by combining high-resolution photocrystallographic experiments with picosecond time-resolved X-ray diffraction experiments. The system studied was α-styrylpyrylium trifluoromethanesulfonate (α-stypy(TFMS)), which has been discussed for application in holographic data storage.[31,34] In the crystalline

(22) Chen, L. X.; Jennings, G.; Liu, T.; Gosztola, D. J.; Hessler, J. P.; Scaltrito, D. V.; Meyer, G. J. *J. Am. Chem. Soc.* **2002**, *124*, 1086.
(23) Gawelda, W.; Johnson, M.; de Groot, F. M. F.; Abela, R.; Bressler, C.; Chergui, M. *J. Am. Chem. Soc.* **2006**, *128*, 5001.
(24) Leibovitch, M.; Olovsson, G.; Scheffer, J.; Trotter, J. *J. Am. Chem. Soc.* **1998**, *120*, 12755.
(25) Theocharis, C. R.; Desiraju, G. R.; Jones, W. *J. Am. Chem. Soc.* **1984**, *106*, 3606.
(26) Harada, J.; Uekusa, H.; Ohashi, Y. *J. Am. Chem. Soc.* **1999**, *121*, 5809.
(27) Kawano, M.; Sano, T.; Abe, J.; Ohashi, Y. *J. Am. Chem. Soc.* **1999**, *121*, 8106.
(28) Hamilton, T. D.; Papaefstathiou, G. S.; MacGillivray, L. R. *J. Solid State Chem.* **2005**, *178*, 2409.
(29) Irie, M.; Kobatake, S.; Horichi, M. *Science* **2001**, *291*, 176.
(30) Chorev, M.; Goodman, M. *Trends Biotechnol.* **1995**, *13*, 438.
(31) Novak, K.; Enkelmann, V.; Wegner, G.; Wagener, K. B. *Angew. Chem., Int. Ed. Engl.* **1993**, *32*, 1614.
(32) Ohba, S.; Hosomi, H.; Ito, Y. *J. Am. Chem. Soc.* **2001**, *123*, 6349.
(33) Mahon, M.; Raithby, P. R.; Sparkes, H. A. *Cryst. Eng. Commun.* **2008**, *10*, 573.
(34) Enkelmann, V.; Wegner, G. *J. Am. Chem. Soc.* **1993**, *115*, 10390.

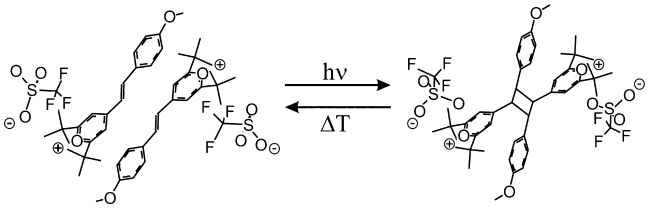

Figure 1. [2+2] cycloaddition reaction of α-stypy(TFMS): left, monomer; right, dimer structure. For the homogeneous single-crystal to single-crystal transformation, optical excitation wavelengths of 520, 550, and 575 nm were used. The back -transformation from the dimer to the monomer is driven by thermal energy. For this, the temperature was set to $T = 370$ K.

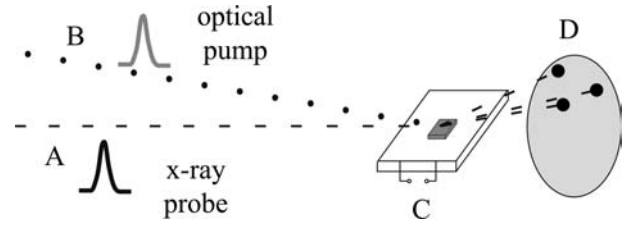

Figure 2. Schematic plot of the grazing incidence setup for the picosecond time-resolved X-ray diffraction experiment. The monochromatized synchrotron X-ray pulses (50 ps pulse width) were selected by a chopper to a frequency of 1 kHz (A). The X-ray beam was focused down to 70 × 200 μm (vertically × horizontally), overlapping with a 500 μm focused optical laser beam (B). The energy of the 100 fs laser pulses (1 kHz repetition frequency) was varied between 1 and 25 μJ, and the wavelength was chosen between 520 and 632 nm. The sample was grown on an electric heating device ($T = 370$ K) (C). The experiment was performed in stroboscopic manner, and the X-ray reflection signals were two-dimensionally collected with an X-ray-sensitive CCD camera (D).

phase, beyond 350 K, the system undergoes a [2+2] photocycloaddition reaction (Figure 1; left, monomer structure, $C_{23}H_{29}O_5SF_3$;, right, dimer structure, $C_{46}H_{58}O_{10}S_2F_6$). At room temperature, the reaction is irreversible; at temperatures higher than 350 K, the cyclobutyl ring opens reversibly. This photoinduced ring-closing mechanism, which is thermally reversible, underlies the Woodward−Hoffmann rule.[35]

Our studies reveal that the product state can be populated and depopulated within picoseconds. During the reaction, the color of the system as well as its dichroic properties change, which makes it an ideal candidate for an organic holographic storage device on very fast time scales.

Experimental Section

Sample Preparation. α-Stypy(TFMS) was synthesized according to ref 36. For the experiments with high spatial resolution, α-stypy(TFMS) crystals with edge lengths of about 200 μm × 150 μm × 150 μm were used. For the diffraction experiments with high temporal resolution, α-stypy(TFMS) crystals with a maximum crystal thickness of 500 nm and edge lengths of 50 μm × 100 μm were investigated. The thickness of the crystals guarantees a homogeneous optical excitation and X-ray probing volume. The crystals were grown on the surface of a metal-covered object holder by recrystallization of the material under slow evaporation of the solvent 1-hexanol.

Optical Spectroscopy. The temperature-dependent back-transformation rates from the yellow dimer crystal to the red monomer crystal were monitored by UV−NIR absorption spectroscopy (Cary-5E spectrometer, 0.2 nm bandpass); further details concerning the spectroscopic setup can be found in ref 37. Crystalline α-stypy(TFMS) was pressed in KBr pellets, and for these experiments the heating option of a closed-loop Oxford cooling system was used. The experiments were performed in 10 K steps between room temperature and 390 K.

The infrared measurements were carried out using a Fourier transform infrared spectrometer (Bruker 5-HR) with a resolution of 0.5 cm^{-1}. The measurements covered an area between 600 and 3500 cm^{-1}. Similarly to the UV−NIR absorption measurement, crystalline α-stypy(TFMS) was pressed in KBr pellets for investigation. The transformation from the monomer to the dimer state was induced by a cold light source at a power of 50 mW for 2 h in a dry N_2 atmosphere to avoid dilution of the sample.

Photocrystallography−Electron Density Analysis. High-resolution photocrystallographic studies of α-stypy(TFMS) single crystals were performed at the F1 and D3 beamlines at the Doris storage ring at Hasylab/DESY. Details about the setups used can be found in refs 38 and 39. An X-ray energy of 20 keV with an X-ray beam size of 0.4 × 0.4 mm^2 was used. The samples were mounted on a four-circle diffractometer (D3) and on a kappa diffractometer (F1). The crystals were measured under the diffraction angles $2\theta = 0°$, $\omega = 90°$, $\chi = 0°$ and $2\theta = 0°$, $\omega = 0°$, $\chi = 10°$ under a full 360° ϕ-rotation in steps of $\Delta\phi = 1°$. Various data sets were collected for different temperatures (10 and 80 K using an open-flow Oxford diffraction Helijet, and at room temperature), and the X-ray diffraction patterns were recorded by the use of a two-dimensional detector (MarCCD165). The monomer crystals reacted to the dimer state by the absorption of 580 nm wavelength from a 1 mm^2 focused cold light source using an OG 580 optical edge filter at a power of 20 mW for 6 h. At low temperatures, the photoreaction was considerably slowed down, allowing high-resolution structural investigations with spatial resolution down to $d = 0.6$ Å. Refinement of the crystal structures of the pure monomer phase and the pure dimer phase is based on about 40 000 reflections. The high data resolution obtained allows for the refinement of the structure up to a level of electron densities. Additionally, the transformation rate of the photoreaction at low temperatures ($T = 100$ K) was recorded. For the mixed crystals, the varying molar fractions of the monomer and dimer phases were determined as a function of illumination time. For these experiments, the samples were irradiated with light at 580 nm and a power of 20 mW, corresponding to the previous experiments.

Picosecond Time-Resolved X-ray Diffraction. The picosecond time-resolved measurements were performed at the ID09B beamline of the ESRF. The setup of this particular experiment in grazing incidence geometry is shown in Figure 2. Further details concerning the general setup of the time-resolved experiment can be found in refs 40 and 41. In the ultrafast experiments, the photoreaction was initiated with 100 fs optical laser pulses which were synchronized/coupled to the synchrotron. A Ti:sapphire laser system with an OPG/OPA (optical parametric amplification) unit was used to generate 520, 550, and 575 nm excitation wavelengths. The chosen optical excitation wavelengths guarantee a homogeneous reaction of the crystal. The optical laser power was systematically varied between 1 and 25 μJ, corresponding to a photon flux of 2 × 10^{13}−5 × 10^{14} photons/pulse. The focal size of the laser on the sample was 0.5−1.5 mm^2. The monochromatic X-ray probe pulse was set to 16.5 keV. The X-ray focal size was 0.2 mm (horizontal) × 0.7

(35) Woodward, R. B.; Hoffmann, R. *J. Am. Chem. Soc.* **1965**, *87*, 395–397.
(36) Hesse, K.; Hünig, S. *Liebigs Ann. Chem.* **1985**, *105*, 715.
(37) Techert, S.; Wiessner, A.; Schmatz, S.; Staerk, H. *J. Phys. Chem. B* **2001**, *105*, 757.
(38) Grabowsky, S.; Pfeuffer, T.; Morgenroth, W.; Paulmann, C.; Schirmeister, T.; Luger, P. *Org. Biomol. Chem.* **2008**, *6*, 2295.
(39) Morgenroth, W.; Overgaard, J.; Clausen, H. F.; Svendsen, H.; Jørgensen, M. R. V.; Larsen, F. K.; Iversen, B. B. *J. Appl. Crystallogr.* **2008**, *41*, 846.
(40) Techert, S.; Schotte, F.; Wulff, M. *Phys. Rev. Lett.* **2001**, *86*, 2030.
(41) Davaasambuu, J.; Durand, P.; Techert, S. *J. Synchrotron Radiat.* **2004**, *11*, 483.

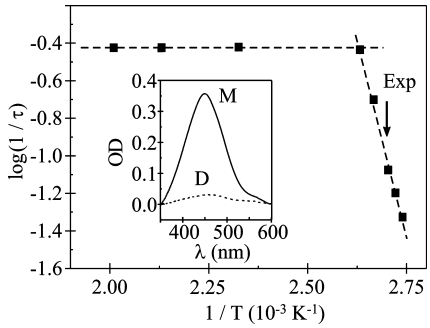

Figure 3. Arrhenius plot of the back-reaction rate, $1/\tau$, of α-styrylpyrylium trifluoromethanesulfonate. The inset shows the absorption spectra of the monomer (red, M) and the dimer (yellow, D) crystal phases. The arrow indicates the temperature setting used for the TR-XRD studies. See the Supporting Information for more details.

mm (vertical) on the sample. For the optical laser pump/X-ray probe excitation geometry a quasi-parallel configuration was used. The X-ray sample geometry was set to grazing incidence. The crystals were measured in rocking scan mode with a rocking range of $\Delta\phi = 2°$, and the reflections were collected with a two-dimensional detector (MarCCD165). The repetition frequency of the whole experiment was 962 Hz. Single X-ray pulses (50 ps long) from the 16 bunch mode were selected by a supersonic running X-ray chopper.

The organic crystals grown on the substrate plates were constantly heated to $T = 370$ K by the use of an electric heating device positioned below the crystals. By this means, it was possible to observe the photoswitching of the system from the monomer to the dimer crystal and back on very fast time scales. Due to the signal-to-noise ratio, it was necessary to integrate over 12 000 shots for each time point. The samples undergo over 1 million switching cycles without any significant radiation damage from the laser beam or synchrotron beam under the given conditions. Due to this resistance to damage, it was possible to use the same samples for measurements at different excitation wavelengths and investigate in this way the influence of the irradiation energy on the dimerization process.

In addition to the Bragg diffraction peaks on α-stypy(TFMS), the electrical heating device shows a diffraction signal which is characteristic for polycrystalline materials. This signal was used to analyze the stability of the synchrotron beam compared to the time-resolved changes of the Bragg diffraction intensities.

Results and Discussion

Spectroscopic Analysis of the Photodimerization in the Crystal. The optical properties of α-stypy(TFMS) during the photoreaction have been characterized by monitoring UV/Vis absorption spectroscopy. Figure 3 summarizes the optical behavior of the system during the photoreaction. The absorption spectra of red crystalline monomer α-stypy(TFMS) and the yellow dimer product are shown in the inset. The monomer has an absorption maximum at 444 nm; meanwhile, the dimer product has no absorption in that range. In the Arrhenius plot, the back-reaction rate τ is plotted as a function of the inverse temperature of the heating device. τ was determined by monitoring the increase of the absorbance at 444 nm as a function of time. At $T = 380$ K, the reaction runs into saturation. For temperatures higher than 500 K, thermal degradation of the system has been observed. For the back-transformation, the Arrhenius analysis reveals an activation energy of $\Delta E_a = 5818$ cm^{-1}. In the figure, the arrow indicates the temperature setting used for the TR-XRD studies. Figure S1 in the Supporting Information shows in detail the changes of the maximum absorption intensity of the monomer band at 444 nm as a function of illumination time.

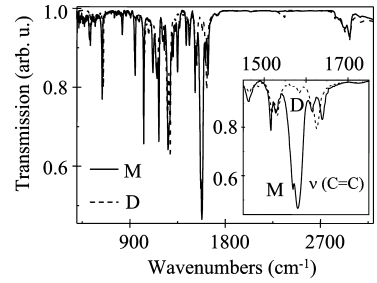

Figure 4. IR transmission spectra of α-stypy(TFMS) in KBr in the monomer (solid line) and dimer phases (dashed line). The strong absorption band at 1580 cm^{-1} corresponds to the stretching mode of the C═C double bond in the monomer molecule. Its disappearance upon illumination is a strong indicator for the dimerization as the C═C double bond opens to form the cyclobutyl ring.

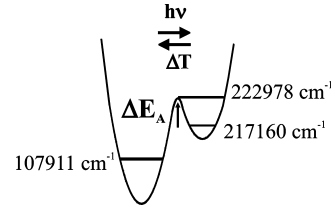

Figure 5. Energy diagram of the photoreaction of α-stypy(TFMS), explaining the principle of its use as a molecular switcher: photoreaction and thermal back-reaction. The activation energy has been determined to be 5818 cm^{-1} above the calculated zero-point energy of 217 160 cm^{-1}.

Under the same experimental conditions as the photocrystallographic experiments, a rate constant of $\tau_{\text{optical}} = 372 \pm 37$ min has been determined.

Besides the optical spectroscopy, infrared measurements of the monomer and dimer crystals were performed in order to prove the dimerization process. Spectra comparing the IR spectra of the monomer and dimer phases are shown in Figure 4. During the dimerization, the stretching mode of the C═C double bond typical for the monomer, ν(C═C) = 1580 cm^{-1}, disappears completely.

Additionally, density functional theory calculations of the monomer and dimer systems[42] have been performed. As an input for the calculations (B3LYP, 6-31 G basis set), the experimental X-ray diffraction data were used after being geometry optimized. The simulations suggest the contribution of about 30 modes to the crystalline cycloaddition reaction: out-of-plane deformation modes (eight $\delta_{\text{symmetric}}$(oop), eight $\delta_{\text{asymmetric}}$(oop)) and out-of-plane and in-plane stretching modes (four $\nu_{\text{symmetric}}$(oop), two $\nu_{\text{asymmetric}}$(oop), four $\nu_{\text{symmetric}}$(ip), four $\nu_{\text{asymmetric}}$(ip)). Based on the spectroscopic results and including the simulations, an energy diagram of the photoreaction of α-stypy(TFMS) as a molecular switcher has been derived (Figure 5). The photoreaction from the monomer to the dimer is instantaneous, and the back-reaction is determined through a thermal activation process. Its activation energy has been determined to be 5818 cm^{-1} above the calculated zero-point energy of 217 160 cm^{-1}. The zero-point energy of the monomer is 107 911 cm^{-1} (with half as many atoms as the dimer).

Data Processing of the X-ray Diffraction Experiments. The X-ray diffraction patterns were analyzed by the use of the software packages XDS[43] and SHELXTL.[44] The refined struc-

(42) Frisch, M. J.; et al. *Gaussian 98*, Revision B.4; Gaussian Inc.: Pittsburgh, PA, 1998.
(43) Kabsch, W. *J. Appl. Crystallogr.* **1993**, *26*, 795.
(44) Sheldrick, G. M. *Acta Crystallogr.* **2008**, *A64*, 112.

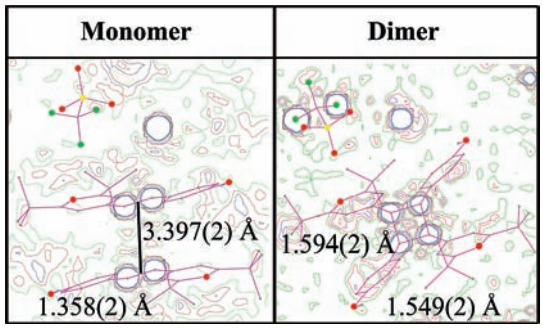

Figure 6. (Left) Electron density map of the pure red monomer phase and (right) electron density map of the pure yellow dimer phase as revealed by photocrystallographic techniques. During the formation of the single bond in the cycloaddition reaction, the distance between two monomer molecules diminishes from 3.397(2) to 1.594(2) Å, and the 1.358(2) Å double bond increases to a 1.549(2) Å C−C single bond. Besides the flipping of the phenyl residues toward the cyclobutyl ring during the addition reaction, the cycloaddition reaction also causes a rotation of the TFMS anion. It should be noted that, already in the monomer phase, the α-stypy(TFMS) molecules stack nearly perfectly on top of each other, forming a quasi-π-complex-like structure.

ture of the monomer phase at 10 K has an $R1$ value of 0.0436 based on 11 722 unique Bragg reflections; w$R2$ is 0.1154, and the GooF value is 1.022. Structural refinement of the dimer phase gives an $R1$ value of 0.0495 using 9834 unique Bragg reflections, a w$R2$ value of 0.1360, and a GooF of 1.059. Additional information on the refinement parameters is given in the Supporting Information.

Electron Density Analysis of the X-ray Diffraction Experiments. The results of high-resolution electron density studies of the monomer and dimer states are presented in Figure 6 (left, electron density map of the pure red monomer phase; right, electron density map of the pure yellow dimer phase). The atoms are printed in CPK colors. The plane of the electron density maps cuts the four interacting carbon atoms in the middle of the molecules. The additional positive contributions of the electron density at the top of both pictures belong to a neighboring molecule of a neighboring plane. Characteristic for the α-stypy(TFMS) system is that, already in the monomer phase, the α-stypy(TFMS) molecules stack nearly perfectly on top of each other, forming a quasi-π-complex-like structure. During the formation of the single bonds in the cycloaddition reaction, the distance between two monomer molecules diminishes from 3.397(2) to 1.594(2) Å, and the 1.358(2) Å double bond increases to a 1.549(2) Å C−C single bond. The intermolecular distance of 3.397 Å is calculated as the arithmetic average of the two intermolecular C═C distances which react with each other during the addition reaction. The chromophoric units on the outer part of the molecules (the phenyl moieties) and the associated TFMS anions compensate the intermolecular distance decrease by their own structural rearrangements: the phenyl moieties flip toward the cyclobutyl ring by about 25°, and the TFMS anion rotates 51° out of the styrylpyrylium plane.

During the photoreaction, the space group of the system remains the same (monoclinic, $P2_1/c$). The structural rearrangements lead to small changes in the metrics (from a(monomer) = 10.23 Å to a(dimer) = 10.83 Å, from b(monomer) = 14.67 Å to b(dimer) = 13.88 Å, from c(monomer) = 15.93 Å to c(dimer) = 16.03 Å, and from β(monomer) = 101.558° to β(dimer) = 105.953°). The number of asymmetric units Z halves from Z(monomer) = 4 to Z(dimer) = 2.

Kinetic Analysis of the X-ray Diffraction Experiments. The photocrystallographic studies with slow kinetic rates have been performed under irreversible reaction conditions, i.e., switching conditions. The dimerization can be monitored by an increase of the lattice parameter β, as shown in the Supporting Information. In Figure S2, the transformation kinetics of the dimerization has been determined to be $\tau_\beta = 350 \pm 20$ min. This value is in agreement with the transformation rate from optical spectroscopic data, which is $\tau_{optical} = 372 \pm 37$ min under comparable excitation conditions.

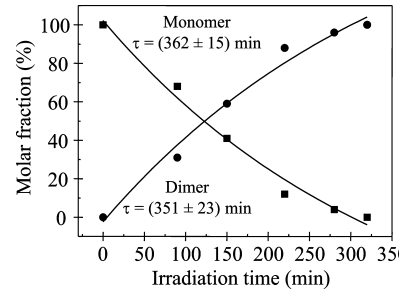

Figure 7. Slow transformation kinetics: time-resolved analysis of the photocrystallographic experiments (580 nm excitation wavelength, 20 mW power). After 350 min of irradiation, the whole crystal has transformed completely from the monomer to the dimer. The determined transformation rates are $\tau_{mono} = 362 \pm 15$ min for the decrease of the monomer molar fraction and $\tau_{dimer} = 351 \pm 23$ min for the increase of the dimer molar fraction. The experiment was performed under irreversible switching conditions.

In a detailed picture of the transformation process, the addition reaction needs to be described by a two-state/two-phase model. The molar fractions of the phototransformed monomer (phase 1) and dimer (phase 2) have been refined according to this two-phase model by comparison of the changes of the measured Bragg diffraction intensity to the structure factors of both pure phases. The molar fraction X(dimer) of the phototransformed dimer phase has been calculated according to[45]

$$X(\text{dimer}) = (I_{tot}/K - |F(\text{monomer})|^2)/(|F(\text{dimer})|^2 - |F(\text{monomer})|^2) \quad (1)$$

where K is the product of the multiplicity, the Lorentz factor, and the polarization factor. According to eq 1, the intensity changes of the Bragg diffraction depend linearly on the number of transformed molecules in the crystal during the phototransformation process. In cases of a phototransformation bigger than 10%, refinement of the molar fraction for both structures is easily feasible.

It should be pointed out that the overall diffraction properties of α-stypy(TFMS) crystals dramatically decreased *during* the phototransformation; meanwhile, very good structures were refined for the pure monomer and the pure dimer phases themselves. It was not possible to refine the structures for mixed crystals on a level of high-resolution electron densities. Nonetheless, it was possible to elucidate the appropriate structures, as been documented (see CIF files of the refined structures in the Supporting Information). After 90 min of irradiation (580 nm excitation wavelength, 20 mW power), the monomer structure was determined with an $R1$ value of 0.136, based on 2413 Bragg reflections to an occupancy of 70%. At the same transformation degree, the dimer structure was refined with an R1 value of 0.152, based on 1273 Bragg reflections (Figure 7). In cases of occupancies less than 10% of one phase, refinement of the minority phase was not carried out. In this transformation,

(45) Techert, S. *J. Appl. Crystallogr.* **2004**, *37*, 445.

the minority phase is located as seeds (with an average domain diameter of less than 10 nm) and originates in diffraction signals with a dramatically enlarged angular fwhm. The presence of a second phase with molar fraction less than 10% causes an increase of the R values when a monophase model is applied. After 300 min of irradiation, the whole crystal has completely reacted from the monomer to the dimer. The transformation rates are $\tau_{mono} = 362 \pm 15$ min for the decrease of the monomer molar fraction and $\tau_{dimer} = 351 \pm 23$ min for the increase of the dimer molar fraction. Again, these values are very well in accordance with the change of the global parameter, which is the angle of the monoclinic unit cell, $\tau_{\beta} = 350 \pm 20$ min, and the transformation time determined in optical spectroscopy, which is $\tau_{optical} = 372 \pm 37$ min.

Switching Process. Experiments revealing the mechanism of ultrafast switching of organic thin films have been performed, which are at the technical limit of what is possible in the field of time-resolved X-ray diffraction today. In order to confirm the results, about 10 thin organic crystalline films, each with different orientations, were investigated in a time-resolved manner. Various parameters were systematically varied, including crystal thickness, temperature for reversible switching, and excitation wavelength. In the following, only the prominent features of the experiment are summarized. In the one-dimensional plot, the time-dependent response function of the integral intensity changes after subtraction of the integral Bragg peak intensities at negative time points (where the laser pump pulse arrives *after* the X-ray probe pulse has been diffracted) is plotted as a function of time.

Figure 8 summarizes a time-resolved sequence of the photoinduced changes of the (121) Bragg diffraction peak of α-stypy(TFMS) organic film in a movie sequence emphasizing the intensity increase and decrease around time zero. As a one-dimensional plot, in Figure 9 the modulation of the integral intensity of the (121) Bragg diffraction peak as a function of optical excitation wavelength and time is representatively summarized. As can clearly been seen in all plots, the integral intensity of the (121) Bragg diffraction peak increases and decreases during the time course of the reaction with an intensity maximum at $t = 0$ ps. For all the experiments, the laser power was set to 15 μJ and the same sample was used.

At 632 nm (Figure 9A), which is outside of the absorption spectrum of α-stypy(TFMS), no photoinduced changes were observed. At 575 nm (Figure 9B), changes on the order of 200 counts (which was about 3% of the total intensity) were just barely observed. At 550 nm excitation wavelength (Figure 9C), the intensity changes increased to 800 counts (10%). The maximum changes were observed at excitation wavelength of 520 nm (Figure 9D, 1500 counts, 20% of the total intensity). The detected intensity changes follow the absorption profile of α-stypy(TFMS): the transformation rate decreases from lower wavelength to higher optical wavelengths. The measurements reveal that the photomodulated signal changes are not affected thermally—they should yield for all optical wavelengths the same intensity changes.

Further confirmation of the ultrafast changes in the structure factor is given in Figure 10, where the photoinduced changes of the (141) Bragg peak (Figure 10A), the (210) Bragg peak (Figure 10B), and the (121) Bragg peak (Figure 10C) are exemplarily presented. In Figure 10A, the α-stypy(TFMS) crystal was excited at 520 nm (25 μJ laser power), in Figure 10B at 520 nm (1 μJ laser power), and in Figure 10C at 550 nm (15 μJ laser power). In summary, the structure factor of the

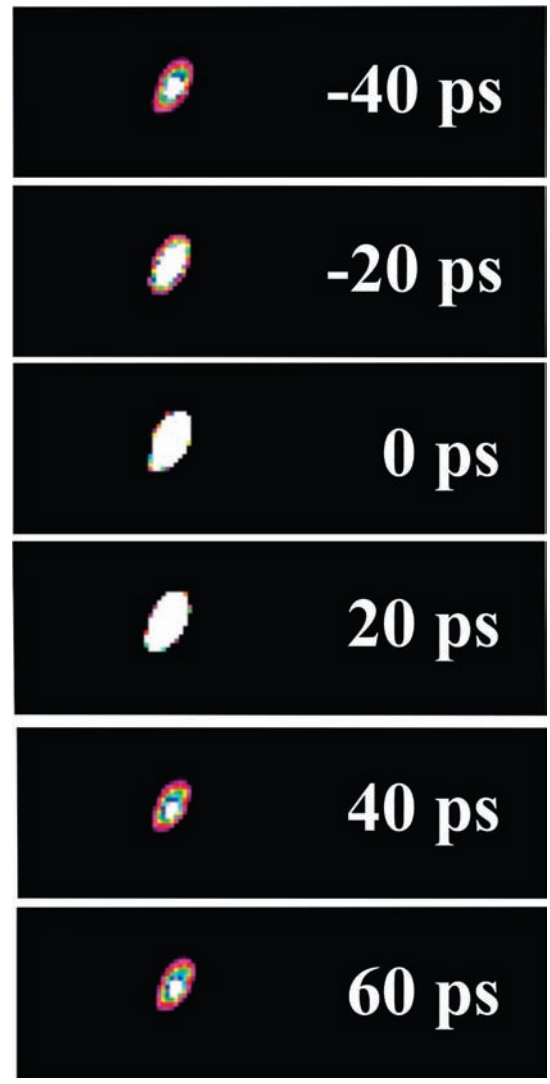

Figure 8. Picoseconds transformation: time-resolved "movie" of the intensity variations of the (012) Bragg diffraction peak upon pulsed laser excitation.

(141) Bragg diffraction peak changes from $|F^{(141)}(\text{monomer})| = 57.83$ to $|F^{(141)}(\text{dimer})| = 78.88$ (intensity increase/decrease); the structure factor for the (210) diffraction changes from $|F^{(210)}(\text{monomer})| = 51.94$ to $|F^{(210)}(\text{dimer})| = 4.76$ (intensity decrease/increase); and the structure factor of the (121) Bragg diffraction peak changes from $|F^{(121)}(\text{monomer})| = 14.05$ to $|F^{(121)}(\text{dimer})| = 58.32$ (intensity increase/decrease).

For the calculation of the ratio between the number of interacting optical photons and the number of reacting molecules in the crystal, the reflection and refraction effects at the incidence angles used were taken into account by applying Snell's law, Fresnel's law, and the Lambert−Beer law. The molar decade extinction coefficients used were determined by optical absorption spectroscopy. With the incidence angles used (from 2° to 17°), a considerable amount of optical radiation is reflected (about 30%) for which the ratio needs to be corrected and finally leads to 1:1 between the number of optical photons and reacting molecules.

Also for the ultrafast experiments, the molar fraction X(dimer) has been calculated according to eq 1. The validity of this approach can be justified by considing that the optical penetration depth of the optical light is $\mu^{-1}(\lambda_{exc} = 520 \text{ nm}) = 780$ nm,

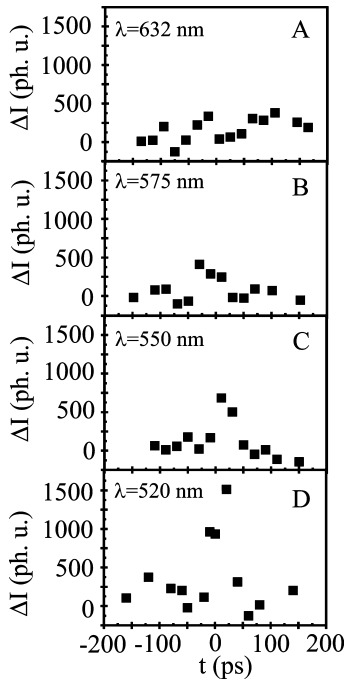

Figure 9. Modulation of the integral intensity of the (012) Bragg diffraction peak as a function of optical excitation wavelength: (A) 632, (B) 575, (C) 550, and (D) 520 nm. The laser power was set to 15 μJ for all measurements. The deviation of the values is at maximum 200 counts, an error within the size of the symbols used.

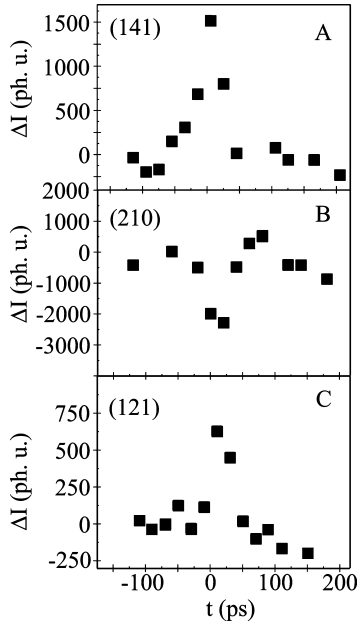

Figure 10. Ultrafast integral intensity modulations of exemplary Bragg diffraction peaks: (A) (141) Bragg diffraction peak (520 nm, 25 μJ); (B) (210) Bragg diffraction peak (520 nm, 1 μJ); and (C) (121) Bragg diffraction peak (550 nm, 15 μJ). The deviation of the values is at maximum 200 counts, an error within the size of the symbols used.

$\mu^{-1}(\lambda_{exc} = 550\ nm) = 2100$ nm, and $\mu^{-1}(\lambda_{exc} = 575\ nm) = 7400$ nm and therefore much bigger than the thicknesses of the crystal films used ($d_{crystal} = 500$ nm), guaranteeing a homogeneous optical excitation. According to this treatment, within 50 ps about 13% (±8%) of the whole crystal thin film has been transformed to the dimer state. The molar fractions were refined on the basis of the analysis of nearly 500 X-ray diffraction peaks. The goodness of the fit was monitored according to

$$R = (\sum ||I_{calc}| - |I_{obs}||/\sum |I_{obs}|) \quad (2)$$

where $I_{calc} = x(F^2_{monomer}) + (x - 1)(F^2_{dimer})$. For the different measurements with various transformation degrees x, R values ranging between 0.08 and 0.1 have been determined.

For the experiments reported, the transformation efficiency is therefore purely limited by the number of optical photons, which was about 10^{11} ph/pulse. An increase in excitation density, however, leads to the generation of photodegradation effects like burning of the organic crystal surface (as been tested various times). The intensity variations found are characterized by a function with nearly symmetric shape (rise times $\tau_{rise} = 20$ ps and decay times $\tau_{decay} = 30$ ps), essentially monitoring the time response function of the ESRF X-ray pulses.

In the following, some remarks about the reaction of the crystal in the molecular switching process will be given. According to the measurements presented to far, the optical excitation of the thin-film crystals was nearly homogeneous. The excitation yield in the crystal, the transformation rate, was limited by the number of optical photons per pulse. One question which arises immediately regards the periodic structural mechanism of the phototransformation in the crystal. If one assumes that the stypy(TFMS) crystals are transformed in an "onion"-like manner, reflecting the intensity profile of the light through the film according to the Lambert−Beer law, domains of 80 nm can be formed during one dimerization cycle. For 16.5 keV X-ray wavelength, the transverse X-ray coherence length is about 17 nm. Each domain formation with dimensions bigger than that coherence length will then be seen as additional Bragg peaks. In particular, Bragg diffraction peaks at higher Miller indices will have the potential spatially to separate. In Figures 11 and 12, such a behavior is reported for the (412) Bragg diffraction peak. As can be seen on the right-hand side from the photocrystallographic measurements, during the photoreac-

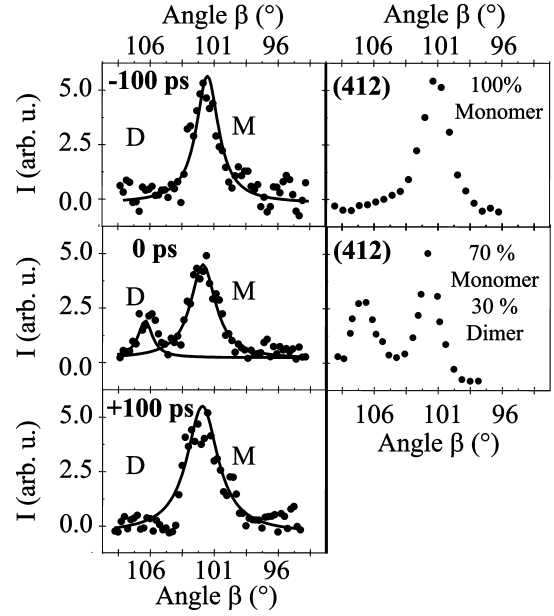

Figure 11. (Left) Ultrafast rise and decrease of the (412) Bragg diffraction peak intensity of the dimer phase for the time points 100, 0, and 100 ps. The splitting of the (412) Bragg diffraction peak for the monomer and dimer phase monitors the changes of the β angle of the monoclinic unit cell from 101.5° to 106°. (Right) As reference, the (412) Bragg diffraction peak for the pure monomer phase and for a mixture of monomer and dimer phases within one crystal (70% monomer, 30% dimer).

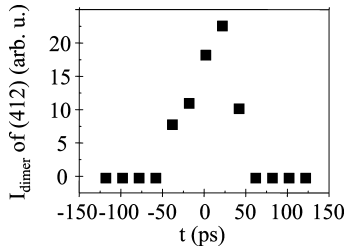

Figure 12. Time-resolved integral intensity modulation of the (412) Bragg diffraction peak for the dimer phase, revealing the fast formation of a dimer domain bigger than 17 nm and its disappearance.

tion (412) splits into two Bragg peaks, one from the monomer and one from the dimer phase (mainly reflecting the changes in the β angle of the monoclinic unit cell due to the dimerization). Comparison to the time-resolved data (Figure 11, left) reveals the same type of behavior for the ultrafast switching process. It is therefore concluded that in the slow transformation as well as in the fast transformation process, the domains formed by the optical excitations are bigger than the coherence length of the X-rays.

Conclusion

Time-resolved X-ray diffraction studied revealed the structural dynamics underlying the molecular switching process of α-stypy(TFMS) upon optical light excitation. The switching process in α-stypy(TFMS) is based on a [2+2] cycloaddition reaction, changing the dichroic properties of α-stypy(TFMS). High-resolution photocrystallographic studies allow for electron density analysis of the overall reaction kinetics. The mechanism of bond-breaking, bond-formation, rearrangement of the neighbor phenyl-moiety, and rotation of the TFMS anion between two states has been revealed. The kinetics could be deduced as a two-state process with changes of the molar fraction of the monomer, respectively dimer phase. The population of the states depends on the number of optical photons and the optical excitation wavelength. Depending on the temperature of the system, for thin crystalline films ultrafast time-resolved grazing incidence experiments proved the reversibility of the photoreaction with time constants faster than 30 ps.

Acknowledgment. This work was supported by SFB 602 and SFB 755 of the Deutsche Forschungsgemeinschaft. Furthermore, S.T. is grateful to the DFG (TE347, 1-3), Aventis Foundation, Fonds of the Chemical Industry, and EU-FLASH MC-8041. J.D. thanks for EU, Grant No. NEST MI-3567. The Advanced Study Group of the Max Planck Society is thanked for continuous support.

Supporting Information Available: Figures S1 and S2, and CIF files. This material is available free of charge via the Internet at http://pubs.acs.org.

JA905484U